Title

Enhancing solar water evaporation with activated carbon

Journal

MRS Advances, 5(50)

ISSN

0272-9172

Authors

Hota, Sai Kiran

Diaz, Gerardo

Publication Date

2020-10-01

DOI

10.1557/adv.2020.267

Peer reviewed

MRS Advances © 2020 Materials Research Society
DOI: 10.1557/adv.2020.267

Enhancing solar water evaporation with activated carbon

Sai Kiran Hota, Gerardo Diaz

School of Engineering, University of California Merced, Merced, CA. 95343

ABSTRACT

Fresh water production through sustainable approaches such as solar thermal sources is attracting widespread attention. One of the recently developed approaches aims at utilizing black particles to enhance evaporation and steam generation through efficient photo-thermal conversion process in direct solar thermal desalination systems. Activated carbon serves as one such material for meeting the objectives of freshwater production with negligible increments in cost of the overall system. A series of chemical and physical characterizations were performed to explore the possibility of using activated carbon as a stable carbon source. Optical characterization showed granular activated carbon to have 96.35% solar absorptance and its dispersion in water to have less than 1.5% transmittance (absorbance of 1.85) at 100 mg/L concentration. Outdoor experiments were performed at the University of California-Merced in the month of September (2019), with peak irradiation of 0.8 suns. The comparative measurements showed that the total evaporation enhancement was 38% and 100% for granular activated carbon and activated carbon dispersions, respectively, when compared to pure DI water.

INTRODUCTION

Water-Energy-Environment nexus has expanded the scope of desalination by means of utilizing renewable sources of energy. Commercial systems such as reverse osmosis (RO), multi-effect desalination (MED), and multi stage flash desalination (MSF), can be powered by sources such as geothermal or solar PV / thermal [1] and these serve as indirect collection systems. Significant contribution has also been aimed at improving productivity of direct solar collection systems such as solar stills, which are more suitable for small residential communities. While research has been aimed at modifying geometry,

the last decade witnessed significant increase in enhancing the photo-thermal property of base fluid by means of nano dispersions and interfacial floating structures. Several materials such as plasmons[2], semiconductors[3], carbon based materials and composites [4,5] have been investigated. Carbon based materials seem to be ideal photo-thermal materials compared to plasmons or composites due to their lower cost and broadband solar absorption spectrum. Numerical studies showed that the optical constants of these materials influenced the photo-thermal conversion potential in the base fluid. Carbon black (CB), carbon nano tubes (CNT's), graphene oxide (GO and reduced GO), have been investigated as suitable carbon materials as both nano dispersions and as solar absorbers for interfacial floating structures[6,7,8,9]. Reported evaporation enhancement has been between 1.5 – 2 times that of water under 1 sun (1 kW) condition with reported evaporation efficiency ranging between 40 and 60%, and with thermal conversion efficiency between 70 and 80%. Contrastingly, the evaporation efficiency of pure (or salt) water is only in the range of 7 to 12%. It was observed that the dispersion concentration positively impacted the evaporation enhancement with intense heat localization at higher concentrations[10,11]. Interfacial floating structures were also developed using these materials as solar absorbers with the aid of thermally insulating, porous, hydrophilic floating structures[12,13,14,15]. Biowaste such as bread, mushrooms, daikon and wood were charred and the resulting products were found to have strong solar absorptance for photo-thermal conversion and evaporation / steam generation enhancement[16,17,18,19]. The primary constraints for these materials are low thermal conductivity, low density, good capillarity and broadband solar absorptance.

It has been observed that the photo-thermal conversion depends strongly on the optical constants in case of dispersions while the structure transmittance and surface reflectance is the key in case of floating structures. Qualitatively, these carbon structures are black in appearance with absorptance higher than 90% and when dispersed in water can increase the fluid absorbance at very small concentration of the material. Activated carbon here is analyzed as one such efficient photo-thermal material. In this paper, a series of physicochemical characterizations were performed to determine the properties of activated carbon as a stable carbon material to improve water evaporation. Outdoor experiments were performed to quantify the evaporation enhancement of water.

MATERIALS AND METHODS

Activated carbon from coconut shell feedstock, in granular and nanoparticle form, were procured from commercial sources. The samples were firstly dried in an oven at 120°C to remove resident moisture and trapped gases. Ultimate analysis was done on the granular sample to determine the Carbon fraction along with Hydrogen, Nitrogen, Sulphur and Oxygen. FT-IR analysis was performed to identify the functional groups in the sample. The density of the sample (skeleton and geometric) along with pore intrusion were obtained to determine the pore content. Raman spectroscopy was performed to identify the crystal structure, while zeta potential was analysed for dispersion stability. Optical characterization was performed on a spin coated glass slide for surface reflectance and transmittance of the sample for use as a solar absorber in bi-layered structures. Similarly, fluid absorbance was determined in the DI water with dispersions.

CHEMICAL CHARACTERIZATION

The activated carbon nanoparticles obtained had a diameter of less than 100 nm and with a purity higher than 95%. The EDX spectrum of the granular activated carbon was collected to qualitatively observe the chemical composition on an environmental scanning electron microscope (FEI Quanta 200ESEM) loaded with an EDX gun. It demonstrated strong presence of Carbon and significant presence of Oxygen along with some impurities.

Table 1 quantifies the breakdown of CHNSO in the granular activated carbon from ultimate analysis. It was observed that carbon constituted more than 94% of the material and almost 2% of the material constituted Oxygen on weight basis. Hydrogen, Nitrogen and Sulphur constituted less than 1% each.

Table 1: Ultimate Analysis for CHNSO breakdown of granular activated carbon

Sample	Carbon (%wt)	Hydrogen (%wt)	Nitrogen (%wt)	Sulphur (%wt)	Oxygen (%wt)
Activated Carbon	94.17	0.5	0.7	0.038	1.9

FT-IR analysis was performed on powdered granular sample and on the nanoparticle sample. The granular samples were crushed on an agate mortar and pestle and passed through a #325 sieve (< 44 μm). The analysis was done on Vertex Bruker70 with the samples placed directly on the ATR diamond crystal. Measurements were recorded at 4 cm^{-1} resolution at 40 scans after eliminating stray data from blank run. Figure 1 shows the FT-IR measurements recorded in attenuated total reflectance (ATR) mode from 4000 cm^{-1} to 400 cm^{-1} wave number range. Both samples were characterized with peaks at 2330 cm^{-1}, 2100 cm^{-1}, 1940 cm^{-1}, and 1570 cm^{-1} corresponding to O=C=O, alkyne (C≡C), allene (C=C=C) and aromatized C=C groups indicating activation [20,21].

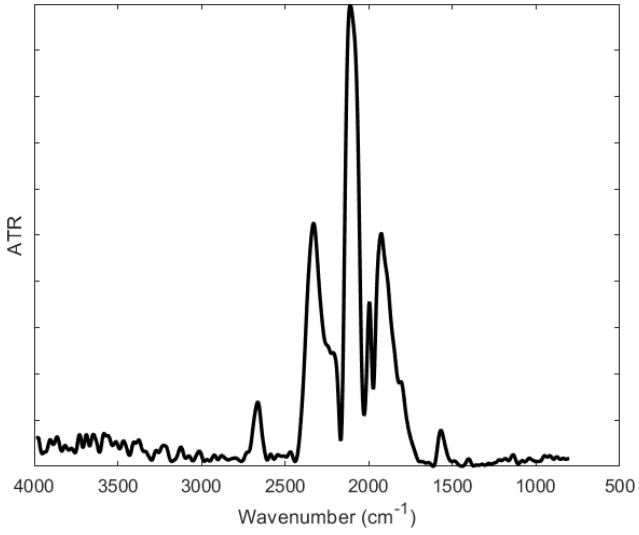

Figure 1: FT-IR spectrum of activated carbon (granular and nanoparticle)

PHYSICAL CHARACTERIZATION

The true (skeleton) and geometric (envelope) density of the granular activated carbon were measured by helium pycnometry and mercury intrusion porosimetry, and were found to be 2106.9 kg/m^3 and 710 kg/m^3, respectively. Accordingly, the measured theoretical porosity was 66% from the calculation (1- 710/2106.9) x 100%. The 532 nm-Raman spectroscopy, as shown in Figure 2 showed activated carbon to be characterized with typical D and G bands of graphitic structure centred around 1340 cm^{-1} and 1600 cm^{-1}. The D band is an indicator of amorphous nature while G band is indicative of crystallinity in the graphite [22]. The Id/Ig (intensity ratio) was observed to be ≈ 1 indicating an intermediate structure. The G band near 1600 cm^{-1} is indicative of higher processing temperature. Powder X-ray diffraction (XRD) performed on PANalytical X'Pert PRO with Cu-Kα corrected from Co-Kα collected at 40 kV and 45 mA further corroborated the turbostratic graphitic structure with a broad amorphous carbon hump at 26° along with 42° (100)/(101) crystalline stacking [23].

Nanoparticle dispersion stability was determined by the zeta potential test carried out in a Malvern Zetasizer nano ZS instrument at dispersion concentration of 100 mg/L. It is suggested that a minimum of $\pm|30|$ mV apparent zeta potential is needed for good stability of the dispersion [24]. Measurements observed in Figure 3, showed that the activated carbon dispersion had a very high stability due to its apparent zeta potential of -47.9 mV.

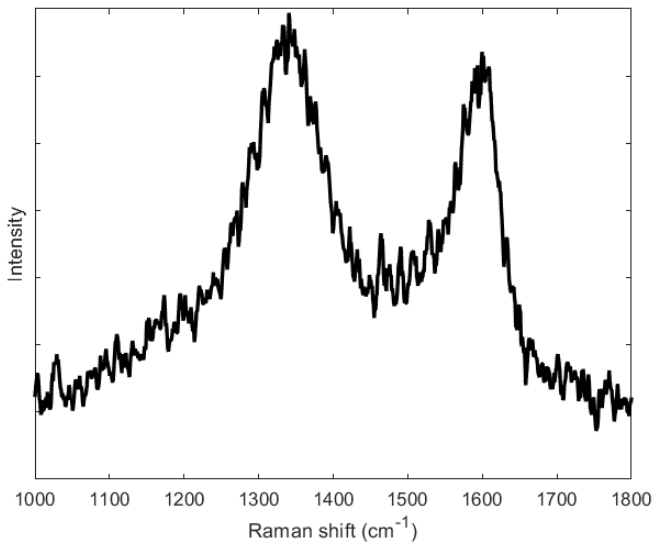

Figure 2: Raman 532 spectrum of activated carbon

OPTICAL INTERACTION

Solar absorptance of activated carbon was calculated from reflectance and transmittance measurements in a SHIMDAZU3600 UV-Vis-NIR spectrophotometer equipped with an integrating sphere in the wavelength (λ) range between 200 nm and 2500 nm. Figure 4 shows the absorptance (A), reflectance (R) and transmittance (T) spectrum measured from the spin coated activated carbon. The absorptance was calculated as A = (1-R-T) x 100%. The weighted average reflectance and transmittance were 3.45% and 0.19%, respectively, indicating the weighted average absorptance to be 96.35%. Similarly, the absorbance of liquid dispersion was measured with 25 mg/L and 100 mg/L concentrations and is shown in Figure 5. The average transmittance (T), through the corresponding dispersions is about 50% for 25 mg/L concentration, while, for 100 mg/L the transmittance is only 1.5% with 10 mm of cuvette path length. The transmittance (T) – absorbance (A) calculation can be given as $A = 2 - \log_{10} T$ (%).

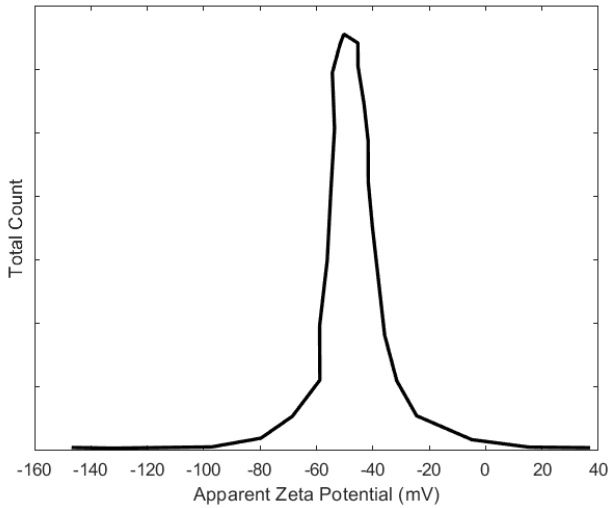

Figure 3: Zeta potential of nanoparticle dispersion

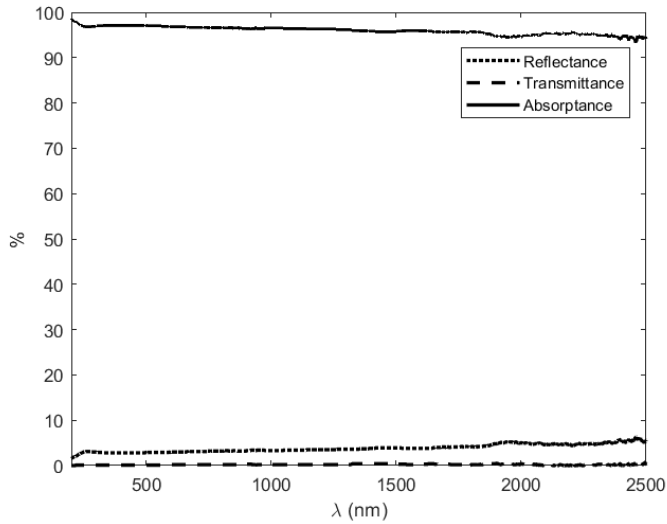

Figure 4: Optical measurements of reflectance, transmittance and absorptance of activated carbon

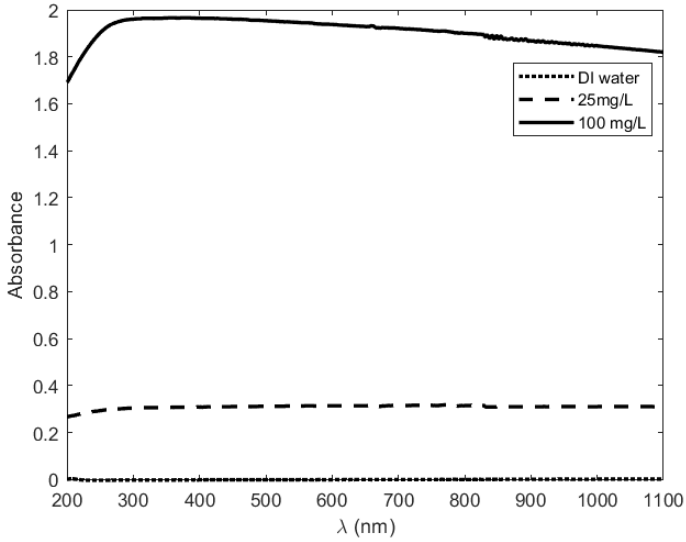

Figure 5: Absorbance of nanoparticle dispersion in DI water

OUTDOOR EXPERIMENTS

Granular activated carbon and nanoparticles were suspended in DI water to test the evaporation enhancement potential under outdoor conditions at UC Merced Castle research facility (32°22' N, 120°34' W) under 0.8 sun peak in the month of September 2019. The ambient temperature increased from 25°C reaching a maximum of 37°C around 3 P.M. Mass loss was measured from glass vials with 30 ml of base fluid (DI water). The suspended granular activated carbon immediately sank to the bottom due to heavy particle density with water filled pores. The nanofluid (100 mg/L concentration) gave a black appearance and was found to be stable from the start at 9:30 AM until the end of the experimental observations at 5 P.M.

The experimental measurements are shown in Figure 6. It was observed that the water evaporated from the glass vials throughout the day under the sunlight, but the evaporation rate was higher in the containers with activated carbon. The total mass loss of water recorded at the end of the day for the glass vials with granular activated carbon and nanoparticles were 2.35 g (1.38 times of DI water) and 3.4 g (2 times of DI water) while that of DI water was only 1.7 g. It is to be noted that the incident solar light heated the whole column of the glass vial instead of normal incidence as is usually done under controlled conditions with a solar simulator.

The calculated peak evaporation rate as shown in Figure 7 between 13:00 P.M – 15:00 P.M were 1.9 kg/m^2-h and 2.5 kg/m^2-h for samples with granular activated carbon and nanoparticles, while that of pure DI water was 1.2 kg/m^2-h. These results are consistent with some of the recently developed solar absorbing materials that have shown 1 sun evaporation rates in the range of 2.06-2.27 kg/m^2-h [25-27] in a controlled atmosphere under solar simulator and closed environment. It is to be noted higher evaporation rate could be a result of higher ambient temperatures. It was noted by Hota and Diaz [10] that higher temperatures result in higher evaporation rates due to increased vapor mass flux gradient. In addition to this, the ambient wind load and relative humidity might have also contributed to measurement of higher evaporation rate.

CONCLUSIONS

Potential for activated carbon for evaporation enhancement of water was investigated. Activated carbon was found to be a carbon rich source with 95% carbon content in both granular and nanoparticle samples. Oxygen was present in the granular sample at almost 2% weight, while, trace presence of other inorganic elements was also detected. The density and pore intrusion measurements showed that the granular activated carbon was highly porous. Raman spectroscopy (532 nm) aided with powder XRD showed that the activated carbon held a turbostratic graphitic structure between graphitic and amorphous phase. The absorptance of activated carbon was found to be higher than 96% which could lead to a strong photo-thermal conversion. Outdoor experiments showed that the total mass loss of water with both granular and nanoparticle activated carbon was higher than that of pure water by 38% and 100%, respectively. Corresponding peak evaporation rate observed for these two samples was 1.9 kg/m^2-h and 2.5 kg/m^2-h, respectively while that for water was 1.2 kg/m^2-h.

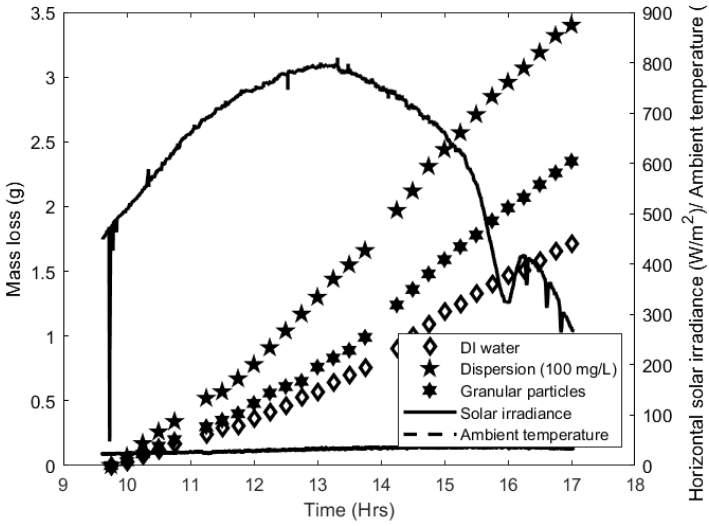

Figure 6: Experimental observation of potential for activated carbon to enhance evaporation of water

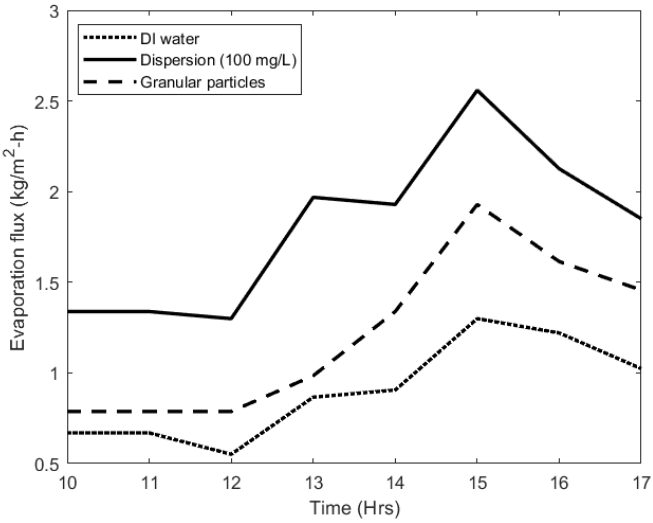

Figure 7: Hourly measured evaporation rate of water through the experiment

ACKNOWLEDGMENTS

Significant portion of the work was supported by funding from California Energy Commission contract #GFO-16-503 and USDA NIFA contract #2-15-67021-24117. Several characterizations were made possible from support of various faculties and staff: Dr. Edhberto Leal Quiros, Dr. Sankha Banerjee, Dr. David Rice, Dr. Anne Kelley, Dr. Yue (Jessica) Wang, Dr. Robert Jordan and Dr. Sarah Kurtz. The authors thank Nathalia Prieto and Riaz Ahamd from Anton-Paar, Kennedy Nguyen (IMF Facility, UC Merced), Jaun Magana from Zalco Labs, Bakersfield and David Garcia and Jon Flores from Nanocomposix.

REFERENCES

[1] E. Mathioulakis, V. Belessiotis and E. Delyannis,"Desalination by using alternative energy: Review and state-of-the-art,," *Desalination*, 203(1-3), 346-365 (2007)

[2] H. Jin, G. Lin, L. Bai, A. Zeiny and D. Wen, "Steam generation in a nanoparticle-based solar receiver," *Nano Energy*, 28, 397-406 (2016).

[3] S. Ishii, R. P. Sugavaneshwar, K. Chen, T. D. Dao and T. Nagao, "Solar water heating and vaporization with silicon nanoparticles at mie resonances," *Optical Society of America*, 6 (2), 640-648 (2016).

[4] B. Hou, Z. Cui, X. Zhu, X. liu, G. Wang, J. Wang, T. Mei, J. Li and X. Wang, "Functionalized carbon materials for efficient solar steam and electricity generation," *Materials Chemistry and Physics*, 222, 159-164 (2019).

[5] Z. Fang, S. Jiao, B. Wang, W. Yin and G. Pang, "A Flexible, Self-Floating Composite for Efficient Water Evaporation," *Global Challenges*, 3, 1800085 (2019).

[6] E. T. Ulset, P. Kosinski and B. V. Balakin, "Solar steam in an aqueous carbon black nanofluid," *Applied Thermal Engineering*, 137, 62-65 (2018).

[7] O. Neumann, A. S. Urban, J. Day, S. Lal, P. Nordlander and N. J. Halas, "Solar Vapor Generation Enabled by Nanoparticles," *ACS Nano*, 7 (1), 42-49 (2013).

[8] G. Ni, N. Miljkovic, H. Ghasemi, X. Huang, S. V. Boriskina, C.-T. Lin, J. Wang, Y. Xu, M. M. Rahman, T. Zhang and G. Chen, "Volumetric solar heating of nanofluids for direct vapor generation," *Nano Energy*, 17, 290-301 (2015).

[9] X. Liu, X. Wang, J. Hunag, G. Cheng and Y. He, "Volumetric solar steam generation enhanced by reduced grpahene oxide nanofluid," *Applied Energy*, 220, 302-312 (2018).

[10] S. K. Hota and G. Diaz, "Activated carbon dispersion as absorber for solar water evaporation: A parametric analysis," *Solar Energy*, 184, 40-51 (2019).

[11] V. Ohri and K. Vikrant, "Using Solar Energy for Water Purification Through Nanoparticles Assisted Evaporation," *Journal of Solar Energy Engineering*, 141 (1), 011008 (2019).

[12] H. Li, Y. He, Y. Hu, Wang and Xinzhi, "Commercially Available Activated Carbon FIber Felt Enables Efficient Solar Steam Generation," *ACS Applied Materials & Interfaces* , 10, 9362-9368 (2018).

[13] X. Wang, Y. He, X. Liu and J. Zhu, "Enhanced direct steam generation via a bio-inspired solar heating method using carbon nanotube films," *Powder Technology*, 321, 276-285 (2017).

[14] Q. Jiang, L. Tian, K.-K. Liu, S. Tadepalli, R. Raliya, P. Biswas, R. R. Naik and S. Singamaneni, "Bilayered Biofoam for Highly Efficient Solar Steam Generation," *Advanced Materials*, 28, 9400-9407 (2016).

[15] Y. Wang, L. Zhang and P. Wang, "Self-Floating Carbon Nanotube Membrane on Macroporous Silica Substrate for Highly Efficient Solar-Driven Interfacial Water Evaporation," *ACS Sustainable Chemistry & Engineering*, 4 (3), 1223-1230 (2016).

[16] Y. Zhang, S. K. Ravi, J. V. Vaghasiya and S. C. Tan, "A Barbeque-Analog Route to Carbonize Moldy Bread for Efficient Steam Generation," *iScience*, 3, 31-39 (2018).

[17] M. Zhu, J. Yu, C. Ma, C. Zhan, D. Wu and H. Zhu, "Carbonized daikon for high efficient solar steam generation," *Solar Energy Materials and Solar Cells*, 191, 83-90 (2019).

[18] N. Xu, X. Hu, W. Xu, X. Li, S. Zhu and J. Zhu, "Mushrooms as Efficient Solar Steam-Generation Devices," *Advanced Materials*, 29, 1606727 (2017).

[19] G. Xue, K. Liu, Q. Chen, P. Yang, J. Li, T. D. J. Ding, B. Qi and J. Zhou, "Robust and Low-Cost Flame-Treated Wood for High-Performance Solar Steam Generation," *ACS Applied Materials & Interfaces*, 9, 15052-15057 (2017).

[20] J. Coates, "Interpretation of Infrared Spectra, A Practical Approach," in *Encyclopedia of Analytical Chemistry*, John Wiley & Sons Ltd, 2000, p. 10815-10837.

[21] C. W. Purnomo, E. P. Kesuma, I. Perdana and M. Aziz, "Lithium recovery spent on Li-ion batteries using coconut shell activated carbon," *Waste Management*, 79, 454-461 (2018).

[22] J. Zhang, F. Lü, H. Zhang, L. Shao, D. Chen and P. He, "Multiscale visualization of the structural and characteristic changes in sewage sludge biochar oriented towards potential agronomic and environmental implication," *Scientific Reports*, 5, 9406 (2015).

[23] B. Manoj and A. G. Kunjomana, "Study of Stacking Structure of Amorphous Carbon by X-Ray Diffraction Technique," *International Journal of Electrochemical Sicence*, 7, 3127-3134 (2012).

[24] V. L. Gaikwad, P. B. Choudhari, N. M. Bhatia and M. S. Bhatia, "Chapter 2 - Characterization of pharmaceutical nanocarriers: in vitro and in vivo studies," in *Nanomaterials for Drug Delivery and Therapy*, William Andrew Publishing, 2019, p. 33-58.

[25] G. Hu, Y. Cao, M. Huang, Q. Wu, K. Zhang, X. Lai, J. Tu, C. Tian, J. Liu, W. Huang, L. Ding, "Salt-Resistant Carbon Nanotubes/Polyvinyl Alcohol Hybrid Gels with Tunable Water Transport for High-Efficiency and Long-Term Solar Steam Generation", Energy Technology, 8, 1900721 (2020).

[26] Q. Zhang, L. Ren, X. Xiao, Y. Chen, L. Xia, G. Zhao, H. Yang, X. Wang, W. Xu, "Vertically aligned *Juncus effusus* fibril composites for omnidirectional solar evaporation", Carbon, 156, 225-233 (2020).

[27] Q. Hou, C. Xue, N. Li, H. Wang, Q. Chang, H. Liu, J. Yang, S. Hu, "Self-assembly carbon dots for powerful solar water evaporation", Carbon, 149, 556-563 (2019).